Nucl. Phys. A 1041 (2024) 122781

Contents lists available at ScienceDirect

Nuclear Physics A

journal homepage: www.elsevier.com/locate/nuclphysa

Measurement of the T_{20} component of tensor analyzing power for the incoherent π^--meson photoproduction on a deuteron

V.V. Gauzshtein [a,*], E.M. Darwish [b,c], A.I. Fix [a], A.S. Kuzmenko [a], M.Ya. Kuzin [a], M.I. Levchuk [d,e], A.Yu. Loginov [f], D.M. Nikolenko [g], I.A. Rachek [g], Yu.V. Shestakov [g,h], D.K. Toporkov [g,h], A.V. Yurchenko [g], B.I. Vasilishin [a], S.A. Zevakov [g], G.N. Baranov [g], A.V. Bogomyagkov [g], V.M. Borin [g], V.L. Dorokhov [g], A.N. Zhuravlev [g], S.E. Karnaev [g], K.Yu. Karyukina [g], A.A. Kovalenko [g], E.B. Levichev [g], I.B. Logashenko [g], S.I. Mishnev [g], I.N. Okunev [g], P.A. Piminov [g], E.A. Simonov [g], S.V. Sinyatkin [g], M.A. Skamarokha [g], E.V. Starostina [g]

[a] National Research Tomsk Polytechnical University, 634050 Tomsk, Russia
[b] Physics Department, College of Science, Taibah University, Medina 41411, Saudi Arabia
[c] Physics Department, Faculty of Science, Sohag University, Sohag 82524, Egypt
[d] Stepanov Institute of Physics, 220072 Minsk, Belarus
[e] Institute of Applied Physics, National Academy of Sciences of Belarus, Minsk, 220072, Belarus
[f] Tomsk State University of Control Systems and Radioelectronics, Tomsk, 634050, Russia
[g] Budker Institute of Nuclear Physics, 630090 Novosibirsk, Russia
[h] Novosibirsk State University, 630090 Novosibirsk, Russia

ARTICLE INFO

Keywords:
Negative pion photoproduction
Tensor analyzing power
Tensor-polarized deuteron

ABSTRACT

We present experimental results for T_{20} component of the tensor analyzing power for incoherent π^- photoproduction on a deuteron. The experiment was performed on an internal tensor-polarized gas deuterium target of the VEPP-3 electron storage ring in 2021 using the proton-proton coincidence method. The data are compared with the results of numerical simulation.

1. Introduction

Study of meson photoproduction on nucleons and nuclei provides us with a powerful tool for investigating strongly interacting matter in the nonperturbative regime of QCD. Use of polarized targets makes it possible to obtain valuable information on the underlying mechanisms and relevant degrees of freedom and, last but not least, to study initial and final state interaction effects.

During the last two decades, experimental measurements of the tensor analyzing power components T_{2M} for photoproduction of the neutral and negative pions on a deuteron have been performed using the internal tensor-polarized deuterium target of the VEPP-3 electron storage ring at the Budker Institute of Nuclear Physics [1–6]. The first measurement of T_{20}, T_{21}, and T_{22} components were reported in Ref. [1]. The data were extracted from the statistics collected in 2003 and have relatively low statistical accuracy.

* Corresponding author.
E-mail address: gauzshtein@tpu.ru (V.V. Gauzshtein).

https://doi.org/10.1016/j.nuclphysa.2023.122781
Received 3 August 2023; Received in revised form 12 October 2023; Accepted 23 October 2023

Available online 25 October 2023

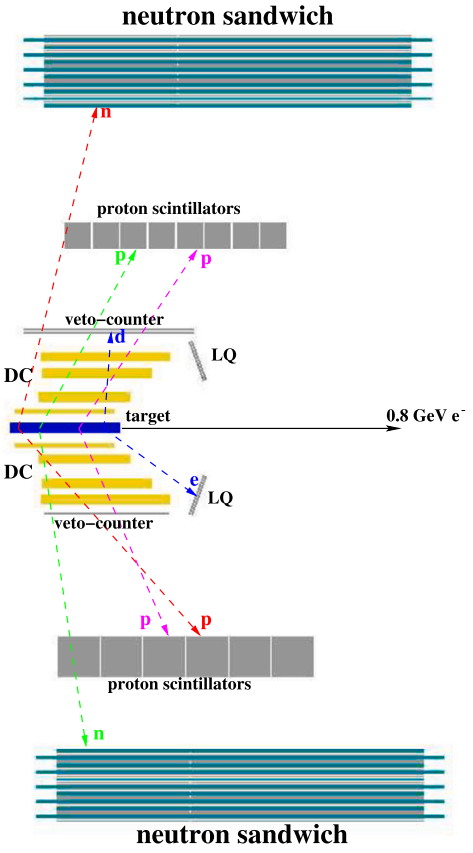

Fig. 1. General scheme of the experiment.

In this paper we present new experimental results for the T_{20} component obtained for the reaction $\gamma d \to pp\pi^-$ in the range of the proton kinetic energy 55 – 160 MeV and the photon energies 300 – 550 MeV. The first preliminary data were reported in Refs. [7,8]. The new data have higher statistical accuracy than those published in [1], but cover a smaller kinematic region.

The paper is structured as follows. In the next two sections the experimental setup and the data analysis are described in some detail. The experimental results and their comparison with a statistical simulation are presented and discussed in Section 4. The summary and conclusion are given in Section 5.

2. Experimental setup

The general scheme of the experiment is shown in Fig. 1. The elements of the detector were placed in the vertical plane above and below the electron beam axis. The energy of the electron beam was 800 MeV. The main goal of the experiment was to study the deuteron two-body photodisintegration $\gamma d \to pn$. That is why the lower and upper arms of the detecting system include both proton and neutron counters. The registration of a proton and neutron in coincidence allows to completely restore the kinematics of the deuteron photodisintegration $\gamma d \to pn$. At the same time, the determination of the kinematic parameters for the two final protons of the reaction $\gamma d \to pp\pi^-$ allows us to study this incoherent process as well.

Each arm of the detecting system includes the drift chambers, charge-veto counters, a layer of proton plastic scintillators and a neutron sandwich calorimeter. For the present analysis the events with a proton detected in the upper proton scintillator in coincidence with a proton detected in the lower proton scintillator have been selected. The proton energy was in the range 55 – 160 MeV. The error of the energy determination did not exceed 15%. The polar and azimuthal angles of the proton emission were measured using the drift chambers in the range $50° - 90°$ and $\pm 30°$, respectively, with an accuracy not worse than $0.6°$.

An open storage cell installed in the VEPP-3 storage ring was used as an internal gas target. Tensor-polarized deuterons were injected into the center of this cell from an atomic beam source (ABS) installed in the median plane of VEPP-3 [9]. The thickness of the internal deuteron target was 3.5×10^{13} at/cm^2. During the data acquisition the sign of the tensor polarization of the deuteron target were reversed every 30 seconds. This duration is three orders of magnitude smaller than the typical time scale of an instability of target density, which is mainly due to a slow degradation of the ABS inner surfaces (see Ref. [9] for details). Thus, the false asymmetry associated with fluctuations in the target density was insignificant, and the absolute value of the target thickness is not required to calculate the asymmetries.

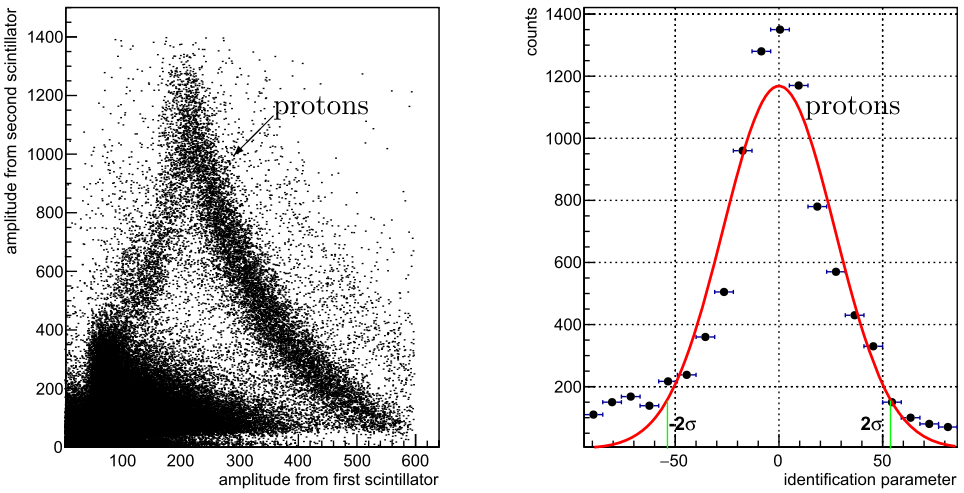

Fig. 2. The left panel is the two-dimensional histogram of the event distributions over the signals from the first and second scintillator of the upper detecting arm. The right panel is the one-dimensional histogram of the event distributions over the proton identification parameter.

The detection of the elastic electron-deuteron scattering at low momentum transfer with the aid of the LQ-polarimeter makes it possible to measure the degree of tensor polarization of the deuteron target during the accumulation of statistics. The design of the LQ-polarimeter was described in detail in Ref. [10]. Despite the almost complete tensor polarization of deuterons ($P_{zz}^{+} \approx +1$ or $P_{zz}^{-} \approx -2$) in the beam at the output of the ABS, the degree of tensor polarization decreases significantly inside the storage cell. The reason for this is the interaction of deuterium atoms with the walls of the storage cell, with each other, and with the pulsed magnetic field of the electron beam in the storage ring. According to the LQ-polarimeter data, the average degree of tensor polarization of the deuteron target, averaged over the entire time of the experiment, was $P_{zz}^{+} = +0.39 \pm 0.025 \pm 0.009$ and $P_{zz} = -1.7\, P_{zz}^{+}$, where the first and the second errors are statistical and systematic, respectively.

3. Data analysis

To identify the events of the reaction $\gamma d \to pp\pi^{-}$, the protons from the lower and upper proton scintillators were detected in coincidence. It is clear that the overwhelming part of the pp-coincidences corresponds to the reaction $\gamma d \to pp\pi^{-}$. In the upper detecting arm, the identification of protons was realized by the $\Delta E/E$ analysis in scintillator layers. The two-dimensional distributions of signals from the scintillators are presented in Fig. 2 on the left. In this plot the first scintillator corresponds to the sum of energy deposition in the thin veto-counters in the upper arm. The second scintillator corresponds to the energy deposition in one of the proton scintillators in the upper arm. As can be seen, the protons form a band whose width is defined by the energy resolutions of the scintillators. Events that do not fall onto the proton band are related either to background processes or to the cases in which the deposition of proton's energy has been distorted. These distortions are associated with an energy loss due to nuclear interactions of protons in the scintillator. On the right in Fig. 2, the distribution of the proton identification parameter is presented. The events that lie in the interval $\pm 2\sigma$ were used for further analysis.

The proton identification method for the lower detecting arm is slightly different. The relationship between the time of flight and the amplitude from the proton scintillator was used in this case. The time of flight is time between hits in the veto-counter and one of proton scintillators from the lower arm. The corresponding histograms are presented in Fig. 3.

In the lower and upper detecting arms, the kinetic energy of protons was reconstructed from the energy deposited in proton scintillators. For an energy calibration, the GEANT4 simulation was used. In our experiment, the scattered electron from the reaction $ed \to e'pp\pi^{-}$ was not detected. However, for the overwhelming majority of events, the polar angle of the electron scattering θ_e was close to zero. Assuming that the electron scattering angle $\theta_e = 0$, and using reconstructed kinematic parameters of the detected protons, we could completely restore the kinematics of the reaction $\gamma d \to pp\pi^{-}$.

To estimate the contribution of the inseparable background to the selected statistics, the GEANT4 simulation using the GENBOS photoreaction generator [11] was performed. Fig. 4 shows the experimental distribution of the reconstructed photon energy together with the corresponding distribution obtained by use the GEANT4 simulation. Fairly good agreement between the experimental and simulation results indicates the correctness of the technique used for reconstructing the kinematic parameters of the reaction $\gamma d \to pp\pi^{-}$.

The main background processes contributing to the pp-coincidences are $\gamma d \to pp\pi^{-}\pi^{0}$, $\gamma d \to pn\pi^{0}$, and $\gamma d \to pn$. The $\gamma d \to pn\pi^{0}$ and $\gamma d \to pn$ processes contribute to the inseparable background because neutrons can knock out protons, which are then detected by proton detectors. The simulation showed that for the photon energy $E_{\gamma} < 550$ MeV, the inseparable background is about 3.4%.

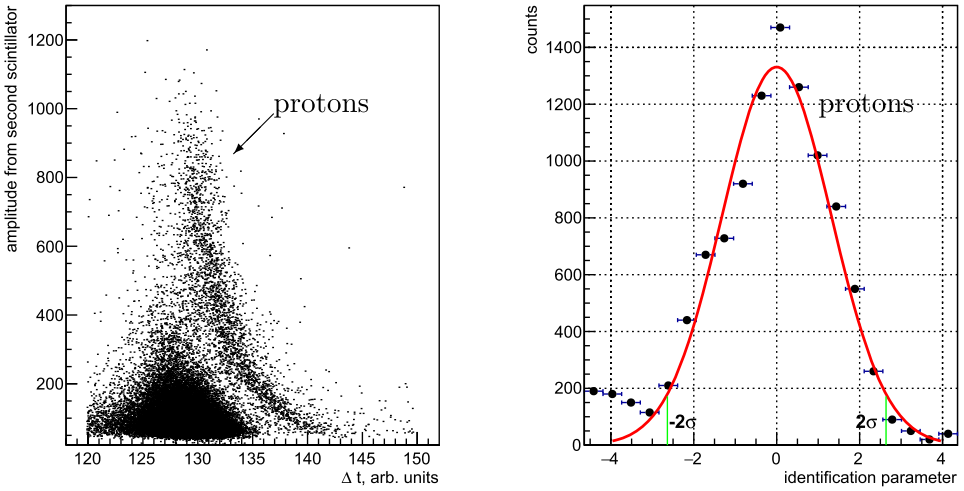

Fig. 3. The left panel is the two-dimensional histogram of the event distributions over the time of flight and the signal from the proton scintillator in the lower detecting arm. The right panel is the one-dimensional histogram of the event distributions over the proton identification parameter.

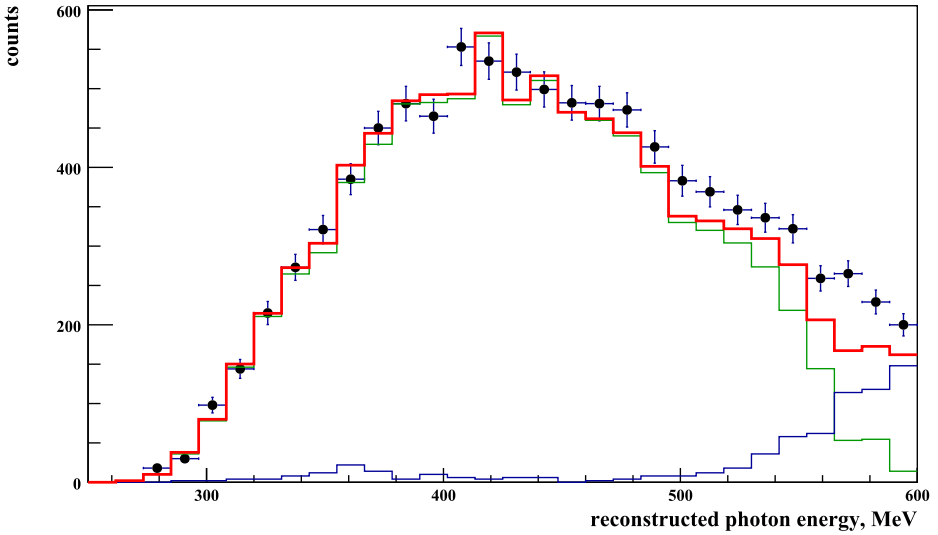

Fig. 4. Distribution of the reconstructed photons energy. The points correspond to the experimental data, the color curves are the results of the GEANT4 simulation: the green curve corresponds to the reaction $\gamma d \to pp\pi^-$, the blue curve corresponds to the background reactions, and the red curve is the sum of the green and blue curves.

4. Results and discussion

In the absence of the vector polarization of the target, the differential cross section for pion photoproduction on a deuteron reads

$$d\sigma = d\sigma_0 \Big\{ 1 + \frac{1}{\sqrt{2}} P_{zz} \big[d^2_{00}(\theta_H) T_{20} - d^2_{10}(\theta_H) \cos(\phi_H) T_{21} + d^2_{20}(\theta_H) \cos(2\phi_H) T_{22} \big] \Big\}, \quad (1)$$

where $d\sigma_0$ is the unpolarized cross section and

$$d^2_{00}(\theta_H) = \frac{3}{2}\cos^2(\theta_H) - \frac{1}{2},$$
$$d^2_{10}(\theta_H) = -\sqrt{\frac{3}{8}}\sin(2\theta_H),$$
$$d^2_{20}(\theta_H) = \sqrt{\frac{3}{8}}\sin^2(\theta_H) \quad (2)$$

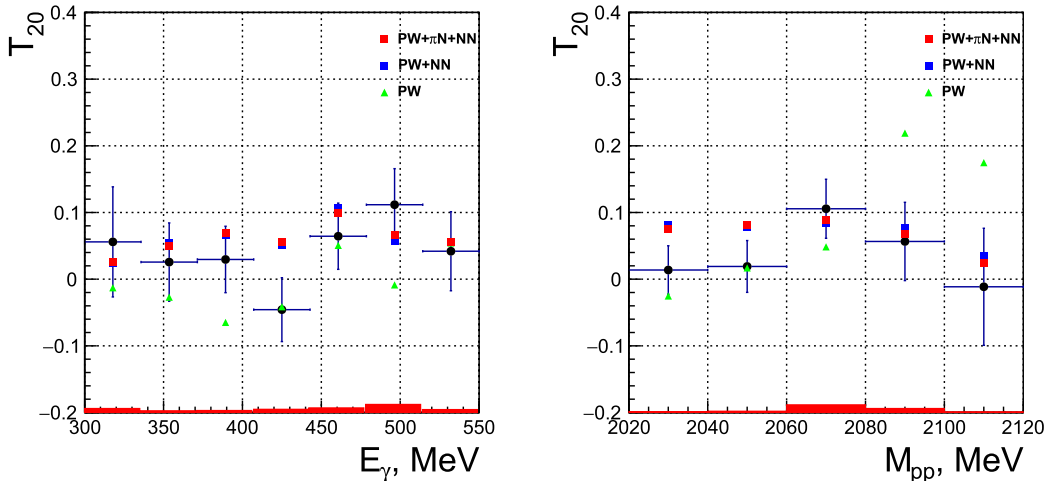

Fig. 5. Dependence of the tensor analyzing power component T_{20} of the reaction $\gamma d \to pp\pi^-$ on the photon energy E_γ and the invariant mass of the pp-system M_{pp}. The data points shown by filled circles represent experimental results of the present experiment, with their error bars are reflecting statistical uncertainties. The red bars underneath each data point reflect its systematic uncertainty. The results of simulation in the plane-wave approximation (green triangles), of the simulation including NN rescattering (blue squares), and of the simulation including πN and NN rescattering (red squares) are also presented.

are the Wigner d-functions. In Eq. (1), the coefficients T_{20}, T_{21}, and T_{22} are the components of the tensor analyzing power of the reaction, P_{zz} is the degree of deuteron tensor polarization, and the angles θ_H and ϕ_H determine orientation of the magnetic field in the coordinate system with the z axis along the photon momentum. The polarization degree P_{zz} can be expressed in terms of the populations n^{s_H} of the deuteron states having spin projections $s_H = -1, 0, +1$ on the magnetic field as:

$$P_{zz} = 1 - 3n^0 = 3(n^+ + n^-) - 2\,. \tag{3}$$

In the experiment, the magnetic field was directed along the photon beam, so that $\theta_H = 0$. As follows from Eqs. (1) and (2), under these conditions only the T_{20} component contributes to the differential cross section. It should also be noted that Eq. (1) is valid only for the coplanar kinematics, when the momenta of all three final particles lie in the same plane.

To separate the contribution from T_{20}, the sign of the tensor polarization was reversed every 30 seconds. Such frequent reversals allow us to suppress systematic errors. Using Eq. (1) one obtains

$$T_{20} = \sqrt{2}\frac{N^+ - N^-}{P_{zz}^+ N^- - P_{zz}^- N^+}\,, \tag{4}$$

where $N^+(N^-)$ is the number of the detected events with the tensor polarization of the target $P_{zz}^+(P_{zz}^-)$.

Our results are presented in Fig. 5 versus the laboratory photon energy E_γ and the invariant mass of the pp system M_{pp}. As may be seen, the measured T_{20} values are quite small, and their magnitude does not exceed 0.1. In Fig. 5, statistic and systematic uncertainties are shown for each data point. The former visibly dominates. The systematic uncertainty mainly comes from the uncertainty in the degree of the deuteron tensor polarization P_{zz}.

To compare experimental results with theoretical predictions, we performed a statistical simulation of the reaction $\gamma d \to pp\pi^-$. To calculate the amplitude, we used the model [12] which includes quasi-free photoproduction on the bound nucleons and takes into account the final state interaction (πN and NN-rescattering). The simulation was performed on the basis of Monte-Carlo algorithm [13,14]. This makes it possible to take into account the complex boundaries of the experimental kinematic domain and an inhomogeneity of the spatial distribution of the deuteron target. The simulated and experimental data have the same structure, in particular, we use the same averaging intervals for the simulated and experimental kinematic variables. This permits one to compare the observed distributions directly to the results of simulation.

The principal results are summarized in Fig. 5 and 6. The green triangles correspond to the amplitude in the plane-wave approximation, the red squares correspond to the amplitude, which also accounts for the πN and NN rescattering in the final state, and the blue squares correspond to the amplitude, which accounts for only the NN rescattering. We see that the final state interaction (FSI) is very important and generally improves the agreement between the experimental and simulated data. Furthermore, the dominant contribution to FSI comes from the NN rescattering, whereas the contribution from the πN rescattering is much less important.

Nevertheless, even after accounting for the FSI corrections, the model is still unable to reproduce the experimental values of T_{20} in some kinematical regions. This especially concerns the results in Fig. 6, where the data demonstrate a sharp variation in the region $130^o \le \Theta_{12} \le 140^o$, whereas the theory predicts rather smooth angular dependence. In this regard, we wish to note that in addition to the πN and NN rescatterings there are other possible corrections, which must also be treated as important additional mechanisms of pion production. These may include $N\Delta$ interaction in an intermediate state of the reaction and contribution of the $\Delta\Delta$ component of the deuteron wave function [15,16]. In addition, a modification of the NN interaction potential at high momentum transfer [17–20] may also visibly affect the components of the tensor analyzing power.

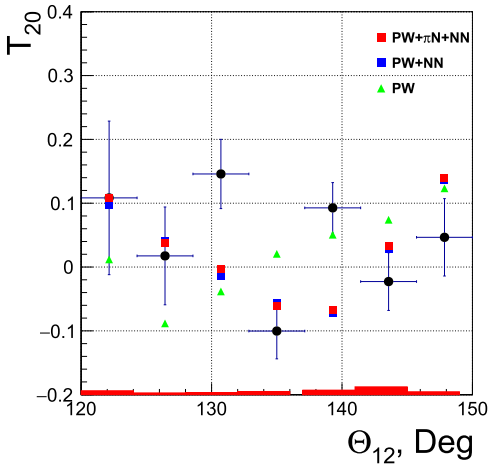

Fig. 6. Dependence of the tensor analyzing power component T_{20} of the reaction $\gamma d \to pp\pi^-$ on the opening angle of two protons. Notations as in Fig. 5.

5. Conclusion

In this work, we have presented the measurement of the T_{20} component of the tensor analyzing power for the reaction $\gamma d \to pp\pi^-$. The results were obtained in the proton energy range 55 – 160 MeV and the photon energy range 300 – 550 MeV. The data obtained are compared with the results of statistical simulations. The first simulation is performed within the plane-wave approximation (PW), the second one also includes the FSI effects (πN and NN-rescattering), and the third one includes only NN-rescattering.

The comparison demonstrates that although the main features of the reaction seem to be well accounted for by the quasi-free mechanism followed by FSI, in some cases we do not achieve satisfactory description of the experimental data. Further improvements in the theoretical treatment including two-body production mechanisms and additional degrees of freedom are needed to achieve a quantitative agreement with the experiment.

CRediT authorship contribution statement

V.V. Gauzshtein: Conceptualization, Investigation, Software, Visualization, Writing – original draft, Writing – review & editing. **E.M. Darwish:** Writing – original draft. **A.I. Fix:** Conceptualization, Investigation, Visualization, Writing – original draft, Writing – review & editing. **A.S. Kuzmenko:** Visualization. **M.Ya. Kuzin:** Visualization. **M.I. Levchuk:** Validation. **A.Yu. Loginov:** Conceptualization, Formal analysis, Investigation, Visualization, Writing – original draft, Writing – review & editing. **D.M. Nikolenko:** Data curation. **I.A. Rachek:** Data curation, Software, Validation. **Yu.V. Shestakov:** Data curation. **D.K. Toporkov:** Data curation. **A.V. Yurchenko:** Data curation. **B.I. Vasilishin:** Data curation. **S.A. Zevakov:** Data curation. **G.N. Baranov:** Data curation. **A.V. Bogomyagkov:** Data curation. **V.M. Borin:** Data curation. **V.L. Dorokhov:** Data curation. **A.N. Zhuravlev:** Data curation. **S.E. Karnaev:** Data curation. **K.Yu. Karyukina:** Data curation. **A.A. Kovalenko:** Data curation. **E.B. Levichev:** Data curation. **I.B. Logashenko:** Data curation. **S.I. Mishnev:** Data curation. **I.N. Okunev:** Data curation. **P.A. Piminov:** Data curation. **E.A. Simonov:** Data curation. **S.V. Sinyatkin:** Data curation. **M.A. Skamarokha:** Data curation. **E.V. Starostina:** Data curation.

Declaration of competing interest

The authors declare that they have no known competing financial interests or personal relationships that could have appeared to influence the work reported in this paper.

Data availability

Data will be made available on request.

Acknowledgements

The data analysis of this work was supported by the Russian Science Foundation, Grant No. 22-42-04401.

References

[1] V.V. Gauzshtein, et al., Nucl. Phys. A 968 (2017) 23.
[2] V.N. Stibunov, et al., J. Phys. Conf. Ser. 295 (2011) 012115.
[3] V.V. Gauzshtein, et al., Phys. At. Nucl. 78 (2015) 1.

[4] S.E. Lukonin, et al., Nucl. Phys. A 986 (2019) 75.
[5] V.V. Gauzshtein, et al., Mod. Phys. Lett. A 36 (2021) 2150199.
[6] I.A. Rachek, et al., Few-Body Syst. 58 (2017) 29.
[7] V.V. Gauzshtein, et al., JETP Lett. 117 (2023) 799.
[8] A.S. Kuzmenko, et al., Atoms 11 (2023) 99.
[9] M.V. Dyug, et al., Nucl. Instrum. Methods A 495 (2002) 8.
[10] M.V. Dyug, et al., Nucl. Instrum. Methods A 536 (2005) 344.
[11] A.S. Iljinov, et al., Nucl. Phys. A 616 (1997) 575.
[12] A.Yu. Loginov, A.A. Sidorov, V.N. Stibunov, Phys. At. Nucl. 63 (2000) 391.
[13] G.I. Kopylov, Zh. Exp. Teor. Fiz. 35 (1958) 1426.
[14] G.I. Kopylov, Zh. Exp. Teor. Fiz. 39 (1960) 1091.
[15] J. Haidenbauer, W. Plessas, Phys. Rev. C 30 (1984) 1822.
[16] J. Haidenbauer, W. Plessas, Phys. Rev. C 32 (1985) 1424.
[17] Yu.F. Smirnov, Yu.M. Tchuvil'sky, J. Phys. G 4 (1978) 1.
[18] V.I. Kukulin, et al., J. Phys. G 27 (2001) 1851.
[19] V.I. Kukulin, et al., Phys. Rev. C 74 (2006) 064005.
[20] V.I. Kukulin, et al., Eur. Phys. J. A 56 (2020) 229.